Investigating the impact of nuclear surface energy coefficients on one-proton radioactivity

R. Gharaei [○],[1,2,][*] Kh. Haghighi Pour,[2] and N. Ghal-Eh [○][2]

[1]*Department of Physics, Sciences Faculty, Hakim Sabzevari University, P.O. Box 397, Sabzevar, Iran*
[2]*Department of Physics, Faculty of Science, Ferdowsi University of Mashhad, P.O. Box 91775-1436, Mashhad, Iran*

The influence of different nuclear surface energy coefficients γ on the process of proton radioactivity is systematically studied within the Coulomb and proximity potential formalism. We investigate the proximity potential Guo 2013 formalism with 13 different versions of the coefficient γ for the description of 44 experimental half-lives of proton emitters in the ground and isomeric states. It has been observed that the four versions, namely Guo 2013 (original), Guo 2013 (set 1), Guo 2013 (set 2), and Guo 2013 (set 3), exhibit the lowest rms deviations (approximately $\sigma = 0.4733$) when compared to the experimental data. The detailed investigation of the known proton decay processes indicate that the decrease in the strength of nuclear surface tension improves the agreement between the experimental data and the calculated values of proton radioactivity half-lives. In addition, our results reveal that the apparent deviation does not follow a continuous behavior around $Z = 68$. In fact, by decreasing the strength of the surface energy coefficient γ compared to its calculated value from the original proximity potential (Guo 2013) for lighter mass regions ($Z < 68$) and increasing it for heavier ones ($Z > 68$), we observe significantly improved agreement with experimental data ($\sigma = 0.453$). A discussion about the role of nuclear surface tension coefficients in the experimental information of proton emitters in the ground state and the isomeric state is also presented.

I. INTRODUCTION

In recent decades, the study of exotic nuclei beyond the β-stability line has become an exciting topic for nuclear physicists. The investigation of these nuclei has led to identifying new radioactive decay modes such as proton emission. In 1970, Jackson *et al.* [1] were the first to discover proton radioactivity from the decay of the isomeric state of ^{53}Co to the ground state of ^{52}Fe by emitting a proton. Since then, with the development of experimental facilities and radioactive nuclear beams, more exotic nuclei have been found to have proton radioactivity from their ground states or low-lying isomeric states. Up to now, about 44 proton emitters (including 29 proton emitters in the ground state and 15 proton emitters in the isomeric state) have been experimentally observed in the mass region $A = 109$ to 185 with the charge numbers between $Z = 53$ to 83. The investigation of proton radioactivity in neutron-deficient nuclei is an invaluable tool for extracting crucial information about nuclear structure. This is because the decaying proton, as the unpaired proton that does not occupy its orbital, offers valuable insights into the nature of these nuclei [2–9]. For example, in Ref. [7] the authors analyzed the role of the quadrupole deformation (β_2) of the parent and daughter nuclei using the interaction potential taken as the sum of the deformed Coulomb potential and deformed proximity potential. They predicted proton decay half-lives for even and odd Z nuclei in the heavy and superheavy region with $Z = 100$–136. It is shown that the Coulomb and

proximity potential model for deformed nuclei (CPPMDN) presents more accurate half-lives for the considered nuclei than the CPPM approach in which both the parent nucleus and daughter nucleus are treated as spherical.

From a physical standpoint, the proton decay radioactivity can be treated in a simple quantum tunneling effect through an effective potential barrier between the emitted proton and the daughter nucleus. On the other hand, this process has the lowest Coulomb potential and highest centrifugal barrier among all charged particles. The semiclassical Wentzel-Kramers-Brillouin (WKB) approximation is a suitable method for describing proton radioactivity due to its ability to account for the quantum mechanical behavior of protons. However, it must be noted that the WKB barrier transmission approximation does not take into account any nuclear structure effects that might influence the proton partial half-life. The spectroscopic factor S_p can be used to described the nuclear structure effects. In fact, this important factor serves as a rich source of information on the fragmentation of a single particle orbital. It is found that there is a link between the quadrupole deformation parameter of the proton emitter and S_p [10]. In addition, the calculations based on the various theoretical approaches (such as the deformed density-dependent model and the generalized liquid drop model) appear to be in good agreement with the measurements by introducing the spectroscopic factors [7,11,12]. Within the framework of the WKB approximation, the emitted proton core interaction potential plays a very important role in calculating the barrier penetrability and thus the proton radioactivity half-lives from various parent nuclei. In recent decades, several theoretical approaches such as the Woods-Saxon (WS) potential [13,14], the single-folding

*Contact author: r.gharaei@hsu.ac.ir; rezagharaei@um.ac.ir

model (SFM) [4], the modified two-potential approach [7,15], the generalized liquid-drop model (GLDM) [11], the effective interactions of density-dependent M3Y (DDM3Y) [12,16], the Gamow-like model (GLM) [17,18], and the Coulomb and proximity potential model (CPPM) [8,19,21] have been proposed predominantly for proton decay studies.

In 1977, Blocki and coworkers [22] suggested the phenomenological proximity potential for estimating the strength of nuclear interactions between two interacting nuclei. The original proximity potential 1977 is based on the proximity force theorem which provides a simple and widely used formula for the nucleus-nucleus interaction potential for studying the properties of the natural radioactivity of different radionuclides and also the fusion of heavy ions; see for example Refs. [23–27]. It is the fundamental advantage of the proximity potential model. Several authors have conducted comparative studies to investigate various types of radioactive decay, including α decay, proton radioactivity, two-proton radioactivity, and heavy particle radioactivity [21,28–30]. These studies have utilized different versions of proximity potential formalisms to analyze and understand the underlying mechanisms of these decay processes. By examining these different formalisms, researchers have been able to gain valuable insights into the behavior of radioactive particles and the factors that influence their decay. In 2019 [21], Deng *et al.* presented a systematic study of the proton radioactivity half-lives of spherical proton emitters using 28 different versions of the proximity potential formalisms. It is found that the Guo 2013 model gives the lowest standard deviations in the description of logarithmic values of experimental proton radioactivity half-lives for the known spherical proton emitters.

This work presents the first systematic observation of the influence of surface energy coefficients on the proton radioactivity process. It is noteworthy that the authors have previously investigated the influence of this physical phenomenon in the fusion of heavy ions [31], α decay [32], and cluster decay of unstable, heavy radioactive nuclei [33]. To achieve our objective, we employ the Guo 2013 proximity potential, considering various versions of surface energy coefficients (γ), to compute the proton-nucleus potential and subsequently determine the half-life of proton transitions from ground states or low-lying isomeric states in 44 proton emitters. A discussion is presented regarding the γ dependence of the standard deviation between the calculated and experimental half-lives of proton radioactivity.

This paper is organized as follows. The details of the calculations of the proton radioactivity half-life and total proton-core interaction potential are provided in Sec. II. The detailed calculations and discussion are presented in Sec. III. The summary and conclusions of the present study are presented in Sec. IV.

II. METHODOLOGY

A. Half-life calculation

The decay constant λ is proportional to the half-life of proton radioactivity as

$$T_{1/2} = \frac{\ln 2}{\lambda}, \qquad (1)$$

here the decay constant λ can be obtained as

$$\lambda = \nu P, \qquad (2)$$

where ν is the assault frequency in relation to the oscillation frequency ω. It can be acquired by

$$\nu = \frac{\omega}{2\pi} = \frac{2E_\nu}{h}. \qquad (3)$$

In this relation, h is the Planck constant. The zero-point vibration energy E_ν is related to the energy of proton radioactivity Q_p [34]. Moreover, P represents the probability of proton penetrating through external barrier and it can be calculated by

$$P = \exp\left[-\frac{2}{\hbar}\int_{r_{\mathrm{in}}}^{r_{\mathrm{out}}}\sqrt{2\mu[V_{\mathrm{tot}}(r) - Q_p]}dr\right], \qquad (4)$$

where $\mu = \frac{m_p m_d}{m_p + m_d}$ denotes the reduced mass of the two-body system with m_d being the daughter nucleus mass and m_p being the proton mass. $\hbar$ is the reduced Planck constant and r is the distance between the centers of the emitted proton and the daughter nucleus. We note that the classical turning points r_{in} and r_{out} can satisfy the conditions $V_{\mathrm{tot}}(r_{\mathrm{in}}) = V_{\mathrm{tot}}(r_{\mathrm{out}}) = Q_p$. The decay energy Q_p is generically calculated by

$$Q_p = \Delta M_p - \left(\Delta M_d + \Delta M_p^\ell\right) + k\left(Z_p^\varepsilon - Z_d^\varepsilon\right), \qquad (5)$$

where ΔM_p, ΔM_d, and ΔM_p^ℓ are the mass excesses of parent and daughter nuclei and emitted proton, respectively. The experimental data of mass excesses ΔM_p and ΔM_d are taken from the recent evaluated nuclear properties table NUBASE2016 [35] and the recent evaluated atomic mass table AME2016 [36,37]. The term $k(Z_p^\varepsilon - Z_d^\varepsilon)$ represents the screening effect of the atomic electrons [38], where $k = 8.7$ eV, $\varepsilon = 2.517$ for $Z \geqslant 60$, and $k = 13.6$ eV, $\varepsilon = 2.408$ for $Z < 60$ [39]. The total interaction potential $V_{\mathrm{tot}}(r)$, between the emitted proton and daughter nucleus, is composed of the nuclear potential $V_N(r)$, Coulomb potential $V_C(r)$, and centrifugal potential $V_\ell(r)$ as

$$V_{\mathrm{tot}}(r) = V_N(r) + V_C(r) + V_\ell(r), \qquad (6)$$

where ℓ is the angular momentum carried away by the emitted proton and can be obtained by the conservation laws of spin and parity. In this paper, we use the proximity potential formalism to determine the emitted proton-daughter nucleus nuclear potential $V_N(r)$. The details are provided in the next section. To calculate the strength of the Coulomb potential $V_C(r)$, we use the following familiar form:

$$V_C(r) = Z_p Z_d e^2 \begin{cases} \dfrac{1}{r} & \text{for } r > R, \\[2mm] \dfrac{1}{2R}\left[3 - \left(\dfrac{r}{R}\right)^2\right] & \text{for } r < R, \end{cases} \qquad (7)$$

where $R = R_p + R_d$. R_d and R_p represent the radii of daughter nucleus and emitted proton, respectively. Z_d and Z_p are the proton number of daughter nucleus and emitted proton, respectively. Note that the calculation formula for $R_{p(d)}$ within proximity potential formalism is given in the next section. As a result of the literature [40], it is necessary to consider a

correction as $\ell(\ell+1) \to (\ell+\frac{1}{2})^2$ for one-dimensional problems. Therefore, we adopt the Langer modified form to obtain the ℓ-dependent centrifugal potential $V_\ell(r)$ as follows:

$$V_\ell(r) = \frac{\hbar^2\left(\ell+\frac{1}{2}\right)^2}{2\mu r^2}, \qquad (8)$$

where μ represents the reduced mass of the proton-daughter nucleus system.

B. The proximity potential Guo 2013 formalism

In 2013, Guo and co-workers [19] introduced a new version of nuclear proximity potential by systematically investigating its universal function for a wide range of fusion reactions based on the double-folding model with the density-dependent (NN) interaction. The authors claimed that the proximity potential formalism with the obtained universal function can reproduce the Coulomb barrier. We mark this modified version as "Guo 2013." According to this model, the nuclear component $V_N(r)$ of the interaction potential can be written as

$$V_N(r) = 4\pi\gamma b \frac{R_p R_d}{R_p + R_d}\Phi(\xi)\ \mathrm{MeV}, \qquad (9)$$

where the nuclear surface width b is assumed close to unity ($b \approx 1$) and the surface energy coefficient γ can be calculated by [20]

$$\gamma = \gamma_0\left[1 - k_s\left(\frac{N-Z}{A}\right)^2\right]\ \mathrm{MeV/fm^2}. \qquad (10)$$

here N, Z, and A represent the neutron, proton and mass numbers of the parent nucleus, respectively. In addition, γ_0 ($= a_2/4\pi r_0^2$, where a_2 is the usual liquid drop model surface energy coefficient and r_0 is the nuclear radius constant) is the surface energy constant and k_s is the surface asymmetry constant. In the present proximity version, $\gamma_0 = 0.9517\ \mathrm{MeV/fm^2}$ and $k_s = 1.7826$. In Eq. (9), R_p and R_d can be provided by

$$R_i = 1.28A_i^{1/3} - 0.76 + 0.8A_i^{-1/3}\ \mathrm{fm}. \qquad (11)$$

The universal function $\Phi(\xi = \frac{r-R_p-R_d}{b})$ is expressed as

$$\Phi(\xi) = \left[\frac{p_1}{1 + \exp\left(\frac{r-R_1-R_p+p_d}{p_3}\right)}\right], \qquad (12)$$

where the adjustable parameters p_1, p_2, and p_3 have the values of -17.72, 1.30, and 0.854, respectively.

III. RESULTS AND DISCUSSION

Over the years, 13 different surface energy coefficients γ have been introduced in the literature [41]. In the present study, we intend to evaluate the interaction potentials and proton radioactivity half-lives of all 44 existing proton emitters (assumed spherical) in the mass region of $A = 109$–185 using the Guo 2013 potential model along with 13 available versions of the γ coefficient. The main data required

TABLE I. The experimental half-lives of the proton emitters in the ground and the isomeric states [35]. The symbol (m) by parent nuclei denotes the isomeric state. The experimental Q_p values calculated by Eq. (5) are taken from Ref. [35] except where noted. The quadrupole deformation parameters β and the spin of the proton moving inside the mother nucleus j_m are from [3,35,47].

Proton emitter	Q_p (MeV)	j_m^π	ℓ	β	$\log_{10} T_{1/2}^{\mathrm{expt}}$ (s)
^{109}I	0.830	$3/2^+$	2[a]	0.160	−3.987
^{112}Cs	0.830	$3/2^+$	2[b]	0.208	−3.310
^{113}Cs	0.981	$3/2^+$	2[b]	0.207	−4.752
^{117}La	0.823[c]	$3/2^+$	2[c]	0.290	−1.623[c]
^{121}Pr	0.901	$3/2^+$	2[b]	0.318	−1.921
^{130}Eu	1.043	$3/2^+$	2[c]	0.331	−3.000
^{131}Eu	0.963	$3/2^+$	2[b]	0.331	−1.703
^{135}Tb	1.193	$7/2^-$	3[b]	0.325	−2.996
^{140}Ho	1.106[c]	$7/2^-$	3[c]	0.297	−2.222[c]
^{141}Ho	1.190	$7/2^-$	3[c]	0.286	−2.387
^{141}Ho$^{\mathrm{m}}$	1.264	$1/2^+$	0[b]	0.286	−5.137
^{144}Tm	1.725[c]	$(5^-, 10^+)$	5[c]	0.255	−5.569[c]
^{145}Tm	1.754	$11/2^-$	5[b]	−0.199	−5.499
^{146}Tm	0.904	$11/2^-$	0[b]	−0.199	−0.810
^{146}Tm$^{\mathrm{m}}$	1.214	$11/2^-$	5[c]	−0.199	−1.125
^{147}Tm	1.133	$11/2^-$	2[b]	−0.190	−3.444
^{147}Tm$^{\mathrm{m}}$	1.072	$3/2^+$	5[b]	−0.190	0.573
^{150}Lu	1.283[c]	$11/2^-$	5[c]	−0.164	−1.194[c]
^{150}Lu$^{\mathrm{m}}$	1.305	$3/2^+$	2[c]	−0.164	−4.398
^{151}Lu	1.255[c]	$11/2^-$	5[c]	−0.156	−0.896[c]
^{151}Lu$^{\mathrm{m}}$	1.335	$3/2^+$	2[b]	−0.156	−4.783
^{155}Ta	1.466	$11/2^-$	5[b]	0.008	−2.495
^{156}Ta	1.036	$3/2^+$	2[b]	−0.050	−0.828
^{156}Ta$^{\mathrm{m}}$	1.126	$11/2^-$	5[b]	−0.050	0.924
^{157}Ta	0.956	$1/2^+$	0[b]	0.045	−0.529
^{159}Re	1.816[c]	$11/2^-$	5[c]	0.064	−4.678[c]
^{159}Re$^{\mathrm{m}}$	1.831[c]	$11/2^-$	5[c]	0.064	−4.695[c]
^{160}Re	1.286	$3/2^+$	2[c]	0.080	−3.164
^{161}Re	1.216	$1/2^+$	0[b]	0.080	−3.357
^{161}Re$^{\mathrm{m}}$	1.336	$11/2^-$	5[b]	0.080	−0.680
^{164}Ir	1.844[c]	$11/2^-$	5[c]	0.089	−3.959[c]
^{165}Ir$^{\mathrm{m}}$	1.737	$11/2^-$	5[b]	0.118	−3.430
^{166}Ir	1.177	2^-	2[b]	0.129	−0.842
^{166}Ir$^{\mathrm{m}}$	1.347	$11/2^-$	5[b]	0.107	−0.091
^{167}Ir	1.087	$1/2^+$	0[b]	0.116	−1.128
^{167}Ir$^{\mathrm{m}}$	1.262	$11/2^-$	5[b]	0.116	0.778
^{170}Au	1.487	2^-	2[b]	−0.105	−3.487
^{170}Au$^{\mathrm{m}}$	1.767	9^+	5[b]	−0.105	−2.975
^{171}Au	1.464	$1/2^+$	0[b]	−0.105	−4.652
^{171}Au$^{\mathrm{m}}$	1.718	$11/2^-$	5[b]	−0.105	−2.587
^{176}Tl	1.278	$(3^-, 4^-, 5^-)$	0[b]	0.075	−2.208
^{177}Tl	1.172	$1/2^+$	0[b]	−0.050	−1.178
^{177}Tl$^{\mathrm{m}}$	1.979	$11/2^-$	6[a]	−0.053	−3.459
^{185}Bi$^{\mathrm{m}}$	1.625	$1/2^+$	0[b]	−0.052	−4.192

[a]Taken from Ref. [35].
[b]Taken from Ref. [17].
[c]Taken from Ref. [5].

for the following calculations are given in Table I. The first column lists the proton emitters. The next three columns represent the Q value of the interaction, the spin of the proton moving inside the mother nucleus, and the angular momen-

TABLE II. The values of the surface energy constant γ_0 and surface asymmetry constant k_s correspond to 13 different versions of the nuclear surface energy coefficients in the proximity potential Guo 2013.

| Proximity version	$\gamma_0(\text{MeV/fm}^2)$	k_s	Ref.
Guo 2013 (original)	0.9517	1.7826	[42]
Guo 2013 (set 1)	0.91144	2.2938	[43]
Guo 2013 (set 2)	0.918	0.7546	[43]
Guo 2013 (set 3)	0.9517	2.6	[44]
Guo 2013 (set 4)	1.01734	1.79	[20]
Guo 2013 (set 5)	1.08948	1.983	[43]
Guo 2013 (set 6)	1.1756	2.2	[45]
Guo 2013 (set 7)	1.2402	3.0	[46]
Guo 2013 (set 8)	1.2496	2.3	[45]
Guo 2013 (set 9)	1.2502	2.4	[45]
Guo 2013 (set 10)	1.25284	2.345	[47]
Guo 2013 (set 11)	1.27326	2.5	[45]
Guo 2013 (set 12)	1.46073	4.0	[48]

FIG. 1. The calculated values of the surface energy coefficient γ using set 1, set 6, set 7, and set 12 in terms of those obtained from the original version γ^{org} for all available proton emitters.

tum, denoted as Q_p, j_m, and ℓ, respectively. The quadrupole deformation parameters β and the experimental proton radioactivity half-life $\log_{10} T_{1/2}^{\text{expt}}$ are given in the fifth and sixth columns, respectively. For ease of calculations, the selected versions of the surface energy coefficient γ are named as those presented in Table II, so that the data can be compared with each other more easily. To facilitate calculations and enhance comparability, the chosen versions of the surface energy coefficients have been assigned names as outlined in Table II. This naming convention allows for a more straightforward comparison of the data among different coefficients. Based on the relationships presented in Eq. (10), it can be easily found that changes in the surface energy constant γ_0 and surface asymmetry constant k_s can produce a change in the strength of the nuclear surface tension between the emitted proton and the daughter nucleus. Under these conditions, we expect that the total proton-core interaction potential and thus the proton radioactivity half-life is found to be affected. However, as pointed out before, the nuclear surface tension concept gets inspiration from the liquid drop model. Additionally, it is essential to recognize that the nuclear potential determines the single-particle energy levels. So the relevant parameters such as the decay energies Q_p derived from the experimental mass formulas can constrain the surface energy coefficient effects on the interaction potential. However, our focus in the present work is on the analysis of the role of the mentioned coefficient on the proton decay process without relying on the role of the Q_p values. In Fig. 1, the behavior of the calculated coefficients γ using four versions, set 1, set 6, set 7, and set 12, are compared with those obtained from the original version γ^{org} for different cases of proton radioactivity isotopes. It should be noted that the selection of these four versions has been done in such a way that it covers the largest, smallest, and two intermediate values of γ_0 among all of the existing versions of the nuclear surface tension coefficient. The behavior of these sets can be generalized to all available versions of the coefficient γ with good accuracy. It is seen in Fig. 1 that each line is located around its corresponding γ_0 constant.
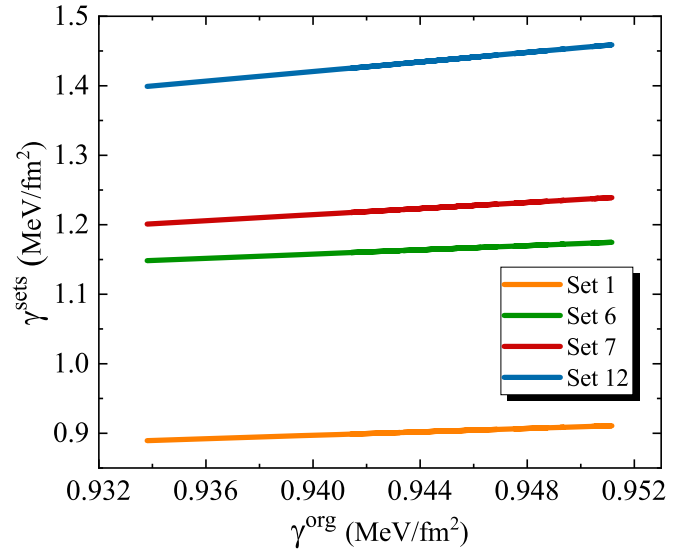
Hence, the effect of this constant on the calculations of the coefficient γ is quite obvious. Furthermore, set 12, which is the furthest line from the x-axis has the greatest difference from the original version. The slope of lines in this figure, on the other hand, can represent the value of k_s in each of the desired sets. The larger the k_s, the steeper the slope. Set 12, for example, shows a steeper slope due to the higher value of its surface asymmetry constant. However, there is a slight difference in the slope of lines. The clearest conclusion that can thus be derived from this figure is that the coefficient k_s has less impact on the calculations compared to the the surface energy coefficient γ_0. By examining the radial behavior of the interaction potential and modifying the strength of the γ coefficient, we can gain valuable insights into the impact of nuclear surface tension effects on the process of proton decay. To achieve this goal, the nuclear and total potentials are calculated for two arbitrary proton decays of ^{145}Tm and ^{155}Ta using the Guo 2013 model along with set 1, set 6, set 7, set 12, and also the original set of the γ coefficient. The results are shown in Fig. 2. As mentioned earlier, Guo 2013 utilizes the microscopic double-folding model in conjunction with realistic density-dependent NN interactions [19]. Therefore, it produces a pocket in the entrance channel potential that is excessively deep. In this situation, it would seem reasonable that we do not analyze the effect of the nuclear surface tension at shorter distances between the reacting nuclei. The important observations from Fig. 2 are as follows: (i) By going from set 1 to set 12 and increasing the power of the γ_0 coefficient (and consequently increasing the nuclear surface tension), the strength of the nuclear attraction between the proton and the daughter nucleus increases. Under these conditions, we expect it to be more difficult to separate the proton from the nucleus. As shown in the figure, only the Guo 2013 proximity model with set 1 provides a more attractive potential than its original version. (ii) In regards to the impact of
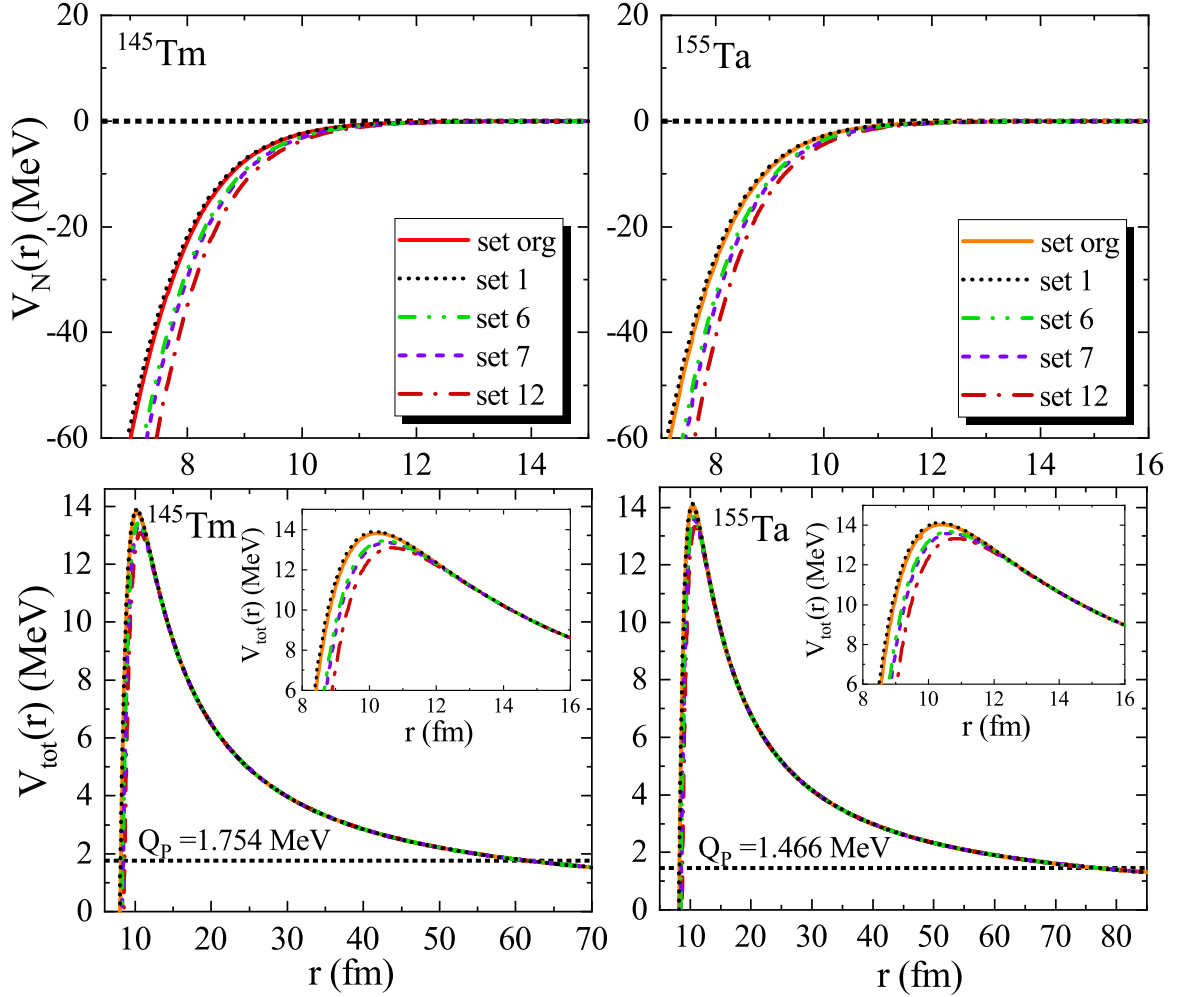
FIG. 2. The behavior of the nuclear $V_N(r)$ and total V_{tot} potentials obtained from five versions of the proximity potentials in terms of the radial distances r (in fm) for proton emitters ^{145}Tm (left panels) and ^{155}Ta (right panels).

γ changes on the Coulomb barrier formed during the decay, the results shown in Fig. 2 demonstrate that an increase in nuclear surface tension leads to a decrease in the barrier height while simultaneously increasing its position. It means that with the increase of γ_0, the total interaction potential curves are shifted to their right side. It is well known that the orbital angular momentum ℓ taken away by the emitted proton is a key quantity in the process of proton radioactivity. The authors demonstrated this subject using different theoretical and experimental approaches [3,9,49–51]. For example, in Ref. [52], the importance of the angular momentum effects has been analyzed by investigating the relationships between the logarithm of the experimental half-lives and $\xi = \frac{Z_d^{0.8}}{\sqrt{Q_p}}$. In the present study, we are interested in exploring the importance of this quantity using the survey of the behavior of the Coulomb barrier positions R_B and barrier heights V_B obtained from the original and modified versions of the Guo 2013 formalism (including γ^{set1}, γ^{set6}, γ^{set7}, γ^{set12}, and γ^{org}) as a function of the surface energy constant γ_0. The results are shown in Fig. 3. We have performed the calculations of this figure for five arbitrary cases of the proton radioactivity isotopes including

Tm, Ta, Re, Ir, and Tl nuclei, which are classified based on the different values of angular momentum $\ell = 0$, 2, 5, and 6. Figure 3 illustrates a clear linear relationship between the calculated values of R_B and V_B with respect to the coefficient γ_0. As the coefficient γ_0 increases, R_B shows a consistent upward trend, while V_B exhibits a steady decline. This observation suggests a strong correlation between the coefficient γ_0 and the variations in R_B and V_B, indicating the significance of this coefficient in determining the behavior of Coulomb barrier characteristics. We can parametrize the observed behaviors using simple formulas as $R_B = a\gamma_0 + b$ and $V_B = a'\gamma_0 + b'$. It is interesting and important to note that the theoretical points with different ℓ are separated in an almost parallel way, but the data with the same ℓ are placed on each other. The effect of the increasing ℓ values on the height of the Coulomb barrier is clearly seen. These results show that angular momentum has a significant effect on the proton emission process. On the other hand, our results reveal that the average values of the slope a (a') and intercept b (b') of the fitted lines get a linear dependence against the angular momentum ℓ. In fact, the average values of the a and b follow respectively an increasing and decreasing trend with increasing ℓ values from
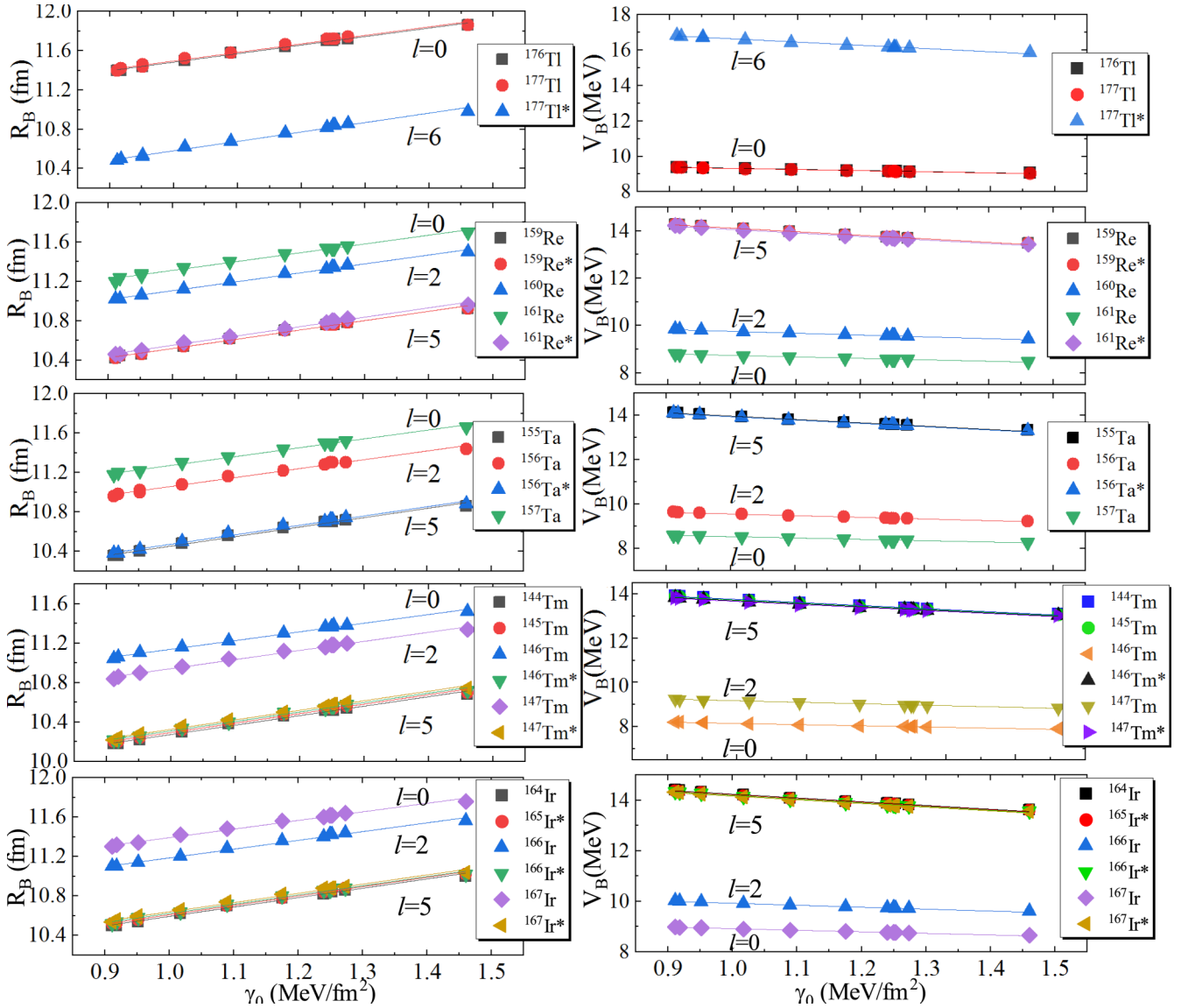
FIG. 3. The behavior of the obtained values for the Coulomb barrier characteristics R_B (left panels) and V_B (right panels) in terms of the constant γ_0 for different isotopes of Tl, Re, Ta, Tm, and Ir using different versions of the surface energy coefficient γ.

$\ell = 0$ to $\ell = 6$. While, the situation in the average values of the slope a' and intercept b' obtained through fitting to the theoretical values of V_B becomes the opposite. Additionally, we can demonstrate that the slope values and intercepts obtained from the linear fits to the plots of the barrier height are more sensitive to changes in the ℓ values than the corresponding values extracted for the barrier position.

It is interesting to explore the effect of nuclear surface tension on the values of barrier penetration probability and proton radioactivity half-life. Again, five versions of the γ coefficient, γ^{set1}, γ^{set6}, γ^{set7}, γ^{set12}, and γ^{org}, are used for the calculations of these two quantities. The values of the barrier penetrability P [Fig. 4(a)] and proton decay half-life $T_{1/2}$ [Fig. 4(b)] obtained from the proximity potential Guo 2013 with set 1, set 6, set 7, and set 12 versions are plotted logarithmically in terms of those obtained within its original

version for all 44 proton emitters. In addition to the above observations, the figures also present a bisector line that illustrates the best fit to the results derived from the initial dataset. It is seen that the points near the bisector line belong to set 1. This means that the theoretical data calculated by this version of the surface energy coefficient are the most consistent with the original version. Additionally, we conclude from an inspection of Fig. 4 that, with the increase of the surface tension coefficient due to the increase in the values of γ_0 from set 1 to set 12, the logarithmic values of the barrier penetration penetrability (half-life of proton emitters) increase (decrease) so that the highest values of $\log_{10} P$ ($\log_{10} T_{1/2}$) are dedicated to set 12 (set 1). These results revealed the fact that there is a direct link between the nuclear surface tension effects and the proton penetration process in the Coulomb potential barrier. Here and in the following we intend to
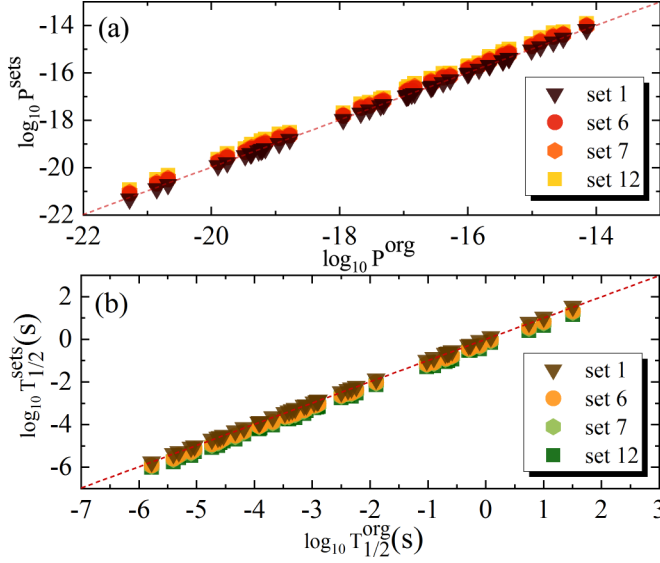
FIG. 4. The logarithmic values of the (a) penetration probability P and (b) half-lives $T_{1/2}$ calculated by the proximity model Guo 2013 along with the γ^{set1}, γ^{set6}, γ^{set7} and γ^{set12} versions in terms of those obtained from the original version of the γ coefficients.
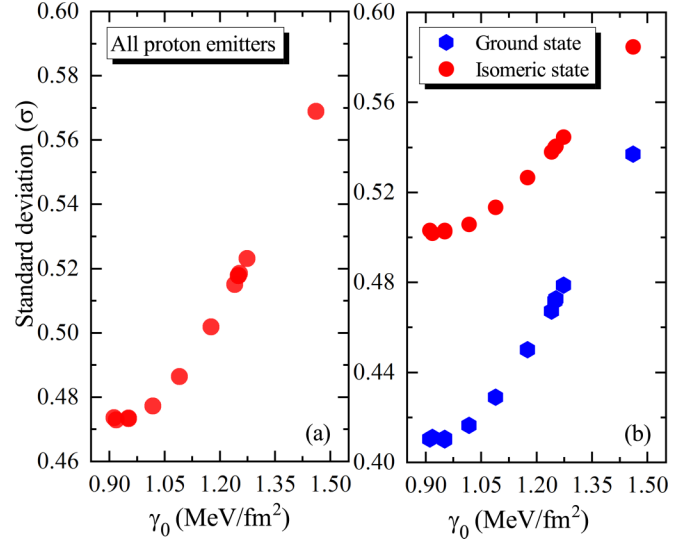

FIG. 5. The behavior of the standard deviation σ in terms of the surface energy constant γ_0 corresponding to 13 versions of the surface energy coefficient (a) for all proton emitters nuclei and (b) for the proton emitters in isomeric and ground states separately.

investigate the effects of changing the γ coefficient on the agreement between theoretical and experimental values of proton radioactivity half-lives for our selected mass range. The standard deviation σ between the logarithmic values of theoretical and experimental data of $T_{1/2}$ can be calculated by

$$\sigma = \sqrt{\frac{1}{n} \sum_{i=1}^{n} \left[\log_{10}\left(T_{1/2i}^{\text{cal}}\right) - \log_{10}\left(T_{1/2i}^{\text{expt}}\right)\right]^2}, \quad (13)$$

where n is the number of parent nuclei. The calculated values σ for Guo 2013 along with different sets of the surface energy coefficient γ are tabulated in Table III. From this table, we clearly see that the values of σ for the proximity potentials with the same values of γ_0 are almost identical.

TABLE III. The standard deviations σ calculated from the Guo 2013 proximity potential along with 13 different versions of the coefficient γ considered in this study.

Proximity version	σ
Guo 2013 (original)	0.4734
Guo 2013 (set 1)	0.4736
Guo 2013 (set 2)	0.4730
Guo 2013 (set 3)	0.4735
Guo 2013 (set 4)	0.4773
Guo 2013 (set 5)	0.4864
Guo 2013 (set 6)	0.5019
Guo 2013 (set 7)	0.5151
Guo 2013 (set 8)	0.5178
Guo 2013 (set 9)	0.5179
Guo 2013 (set 10)	0.5185
Guo 2013 (set 11)	0.5232
Guo 2013 (set 12)	0.5690

For instance, we can refer to the original version of the Guo 2013 formalism, as well as its modified forms, namely Guo 2013 (set 1), Guo 2013 (set 2), and Guo 2013 (set 3). These modified versions have been found to yield the lowest values of the standard deviation (approximately $\sigma = 0.4733$) when describing the experimental proton radioactivity half-lives.

This result holds also true for the Guo 2013 (set 7), Guo 2013 (set 8), Guo 2013 (set 9), and Guo 2013 (set 10) formalisms with average value $\sigma = 0.5173$. Another point to note in Table III is that the value of σ for the proximity potential Guo2013 formalism with set 12 is maximum. This indicates that this version is not suitable to deal with proton radioactivity. In addition, it is easy to see that the change in the k_s values plays a minor role in the theoretical half-lives of proton radioactivity. This result can be demonstrated by comparing the standard deviations σ of the original set ($\gamma_0 = 0.9517$ MeV/fm^2, $k_s = 1.7826$) and set 3 ($\gamma_0 = 0.9517$ MeV/fm^2, $k_s = 2.6$). Consequently, it seems that the agreement with experimental data is sensitive to the change in the strength of nuclear surface tension. In order to investigate this point, we plot in Fig. 5 (left panel) the trend of the calculated values of the standard deviation σ as a function of the coefficient γ_0 for all the known proton emitters. From this figure, we can find that the agreement with the experimental data improves by decreasing the values of γ_0. In Fig. 5 (right panel), as in panel (a), we display the variation of σ against the surface energy constant γ_0 but separately for proton emitters in the ground states and isomeric states. From the figure, we see that the results obtained for the proton emitters in the ground state are more sensitive toward the values of γ_0 than those obtained for isomeric states; in such a way that it seems that the calculated values of the standard deviations manifest the tendency to develop a convergent behavior at large nuclear surface tensions. Additionally, we find that the various versions of proximity potential formalisms considered
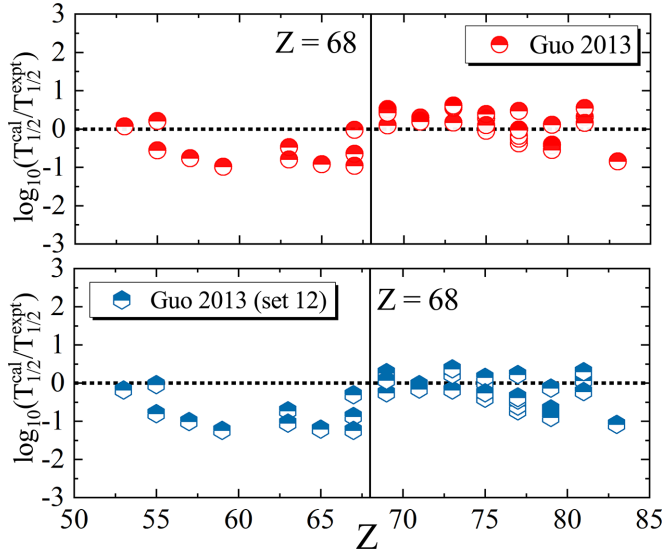
FIG. 6. The logarithmic differences between $T_{1/2}^{cal(sets)}$ and $T_{1/2}^{expt}$ in terms of atomic number Z obtained from the γ^{org} and γ^{set12} versions.

TABLE IV. The calculated values of the standard deviations σ for nuclei before and after $Z = 68$ separately.

γ_0 (MeV/fm^2)	σ (for $Z < 68$)	σ (for $Z > 68$)
0.91144	0.6473	0.3993
0.918	0.6518	0.3958
0.9517	0.6692	0.3867
0.9517	0.6686	0.3872
1.01734	0.7027	0.3731
1.08948	0.7377	0.3662
1.1756	0.7771	0.3668
1.2402	0.8044	0.3716
1.2496	0.8088	0.3735
1.2502	0.8089	0.3734
1.25284	0.8100	0.3739
1.27326	0.8186	0.3764
1.46073	0.8901	0.4094

here are more suitable to describe the experimental information on ground state proton emitters than the isomeric ones. This result can indicate the need for taking into account the thermal effects of hot parent nuclei in the calculation of proton emission half-lives through a modified temperature-dependent surface energy coefficient [53].

In 2006 [3], Delion and coworkers analyzed the dependence of the quadrupole deformation parameter β upon the charge number Z for proton emitters with $Z > 50$. The results show that a sudden change in the nuclear shape occurs at $Z = 68$ which is independent of the angular momentum of the outgoing proton. Accordingly, the authors indicated that the logarithm of the experimental half-lives corresponding to proton decay lie on two straight lines, and thus presented a simple formula for these data. Our results using the various versions of the proximity potential Guo 2013 formalism reveal that the difference between the logarithmic values of $T_{1/2}^{cal}$ and $T_{1/2}^{expt}$ appears to be discontinuous around the proton number $Z = 68$. An example is shown in Fig. 6 for the original version of Guo 2013 and its modified form Guo 2013 (set 12). As can be seen from this figure, in order to improve the data quality, the calculated half-lives before $Z = 68$ should be moved up to the zero line, and those lying within $Z > 68$ should often be moved down. That is why the idea of a piecewise function for the surface energy coefficient γ can be proposed, where one part deals with $Z < 68$ and the other deals with $Z > 68$. To introduce this function, we calculate separately the standard deviations σ in both regions $Z < 68$ and $Z > 68$; see Table IV. The result of this will be to find the best version of the surface energy coefficient to reproduce the experimental data of proton radioactivity half-lives in each of these regions. Depending on Table IV, set 1 (with $\gamma_0 = 0.911\,44$) and set 5 (with $\gamma_0 = 1.089\,48$) versions produce the lowest value of σ for parent nuclei in regions $Z < 68$ and $Z > 68$, respectively. This means that in comparison with the original version of the coefficient γ, we need to reduce and enhance the strength

of nuclear surface tension in the mass regions $Z < 68$ and $Z > 68$, respectively. Under these conditions, we suggest a modified form of Eq. (10) to deal with the proton radioactivity within the proximity potential formalism as follows:

$$\gamma(\gamma_0', k_s') = \gamma_0' \left[1 - k_s' \left(\frac{N - Z}{A} \right)^2 \right], \quad (14)$$

with

$$\gamma_0' = 0.91144, \quad k_s' = 2.293 \quad \text{for } Z < 68,$$
$$\gamma_0' = 1.08948, \quad k_s' = 1.983 \quad \text{for } Z > 68. \quad (15)$$

The standard deviation σ calculated by Eq. (14) for all the considered nuclei is $\sigma = 0.4531$. This means that the presently obtained function for the surface energy coefficient in proximity potential Guo 2013 can slightly improve the agreement with the experimental data by about 5%. Interestingly, we analyze the dependence of the standard deviation on
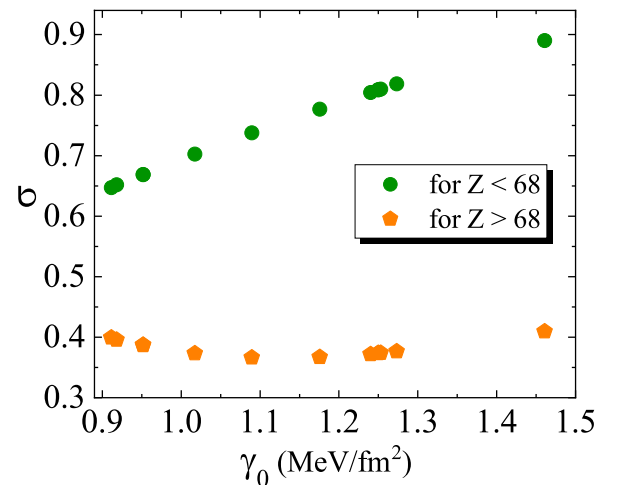

FIG. 7. The behavior of the standard deviation σ in terms of the surface energy constant γ_0 corresponding to the mass regions $Z < 68$ and $Z > 68$.

the value of the coefficient γ_0. Results are shown in Fig. 7 for different sets of the surface energy coefficient in regions $Z < 68$ and $Z > 68$. From this figure, one can find that the proximity potential Guo2013 formalism performs better for heavier nuclei ($Z > 68$) than lighter ones ($Z < 68$). On the other hand, it is seen that the calculations of proton radioactivity half-lives have a strong dependence upon the nuclear surface tension effects for parent nuclei in region $Z < 68$, whereas the values of σ are less sensitive toward the coefficient γ_0 for heavier proton emitters ($Z > 68$). Physical justification for the present result comes from this reality that the nucleus area reduction during proton radioactivity leads to an increase in the γ_0 constant and resulting in the surface energy coefficient γ [54].

IV. CONCLUSIONS

To summarize, we perform a systematic study analyzing the influence of different nuclear surface energy coefficients of the proximity potential on proton radioactivity. In order to achieve our objective, we employ 13 distinct variations of the surface energy coefficients in the proximity potential Guo 2013 formalism. This approach enables us to accurately calculate the proton radioactivity half-lives of 44 proton emitters. We have tried to demonstrate in this work that,

compared to the surface energy constant γ_0, the surface asymmetry constant k_s has a negligible influence on the half-lives of proton decay processes. By analyzing the behavior of the calculated barrier heights and positions with the coefficient γ_0, we indicate the importance of the contributions of the orbital angular momentum ℓ on the proton decay process. Our study reveals the dependence of the barrier penetration probability P and proton radioactivity half-life $T_{1/2}$ on the nuclear surface tension effects. It is shown that the calculated values of P and $T_{1/2}$ were found to increase and decrease with increase in strength of nuclear surface tension between two interacting nuclei, respectively. In addition, we found that the agreement between the experimental data and the calculated values of half-life of proton radioactivity increase by decreasing the values of nuclear surface energy coefficients. On the basis of the existence of the jump occurring at $Z = 68$, a very simple formula is presented for calculating the nuclear surface energy coefficients used in the proximity potential. We would like to point out that this formula enables one to reproduce the experimental proton radioactivity half-lives with acceptable accuracy. Our calculated results also reveal that one needs to apply a temperature-dependent form of the interaction potential to provide a more accurate description of the experimental information on isomeric state proton emitters.

[1] K. P. Jackson, C. U. Cardinal, H. C. Evans, N. A. Jelley, and J. Cerny, Phys. Lett. B **33**, 281 (1970).

[2] A. A. Sonzogni, Nucl. Data Sheets **95**, 1 (2002).

[3] D. S. Delion, R. J. Liotta, and R. Wyss, Phys. Rev. Lett. **96**, 072501 (2006).

[4] D. N. Basu, P. R. Chowdhury, and C. Samanta, Phys. Rev. C **72**, 051601(R) (2005).

[5] B. Blank and M. Borge, Prog. Part. Nucl. Phys. **60**, 403 (2008).

[6] H. F. Zhang, Y. J. Wang, J. M. Dong, J. Q. Li, and W. Scheid, J. Phys. G: Nucl. Part. Phys. **37**, 085107 (2010).

[7] Y. Qian and Z. Ren, Eur. Phys. J. A **52**, 68 (2016); K. P. Santhosh and I. Sukumaran, *ibid.* **54**, 102 (2018).

[8] K. P. Santhosh and I. Sukumaran, Phys. Rev. C **96**, 034619 (2017).

[9] R. Budaca and A. I. Budaca, Eur. Phys. J. A **53**, 160 (2017).

[10] D.-M. Zhang, L.-J. Qi, H.-F. Gui, S. Luo, B. He, Xi.-J. Wu, and X.-H. Li, Phys. Rev. C **108**, 024318 (2023).

[11] J. M. Dong, H. F. Zhang, and G. Royer, Phys. Rev. C **79**, 054330 (2009).

[12] Y. B. Qian, Z. Z. Ren, and D. D. Ni, Chin. Phys. Lett. **27**, 030508 (2010).

[13] J. Dudek, Z. Szymanski, and T. Werner, Phys. Rev. C **23**, 920 (1981).

[14] B. Buck, A. C. Merchant, and S. M. Perez, Phys. Rev. C **45**, 1688 (1992) 12.

[15] J.-H. Cheng, J.-L. Chen, J.-G. Deng, X.-H. Li, Z. Zhang, and P.-C. Chu, Nucl. Phys. A **997**, 121717 (2020).

[16] M. Bhattacharya and G. Gangopadhyay, Phys. Lett. B **651**, 263 (2007).

[17] A. Zdeb, M. Warda, C. M. Petrache, and K. Pomorski, Eur. Phys. J. A **52**, 323 (2016).

[18] J. L. Chen, X. H. Li, J. H. Cheng, J. G. Deng, and X. J. Wu, J. Phys. G: Nucl. Part. Phys. **46**, 065107 (2019).

[19] C. L. Guo, G. L. Zhang, and X. Y. Le, Nucl. Phys. A **897**, 54 (2013).

[20] W. D. Myers and W. J. Swiatecki, Nucl. Phys. **81**, 1 (1966).

[21] J. G. Deng, X. H. Li, J. L. Chen, J. H. Cheng, and X. J. Wu, Eur. Phys. J. A **55**, 58 (2019).

[22] J. Błocki, J. Randrup, W. J. Świątecki, and C. F. Tsang, Ann. Phys. (NY) **105**, 427 (1977).

[23] Y. J. Yao, G. L. Zhang, W. W. Qu, and J. Q. Qian, Eur. Phys. J. A **51**, 122 (2015).

[24] R. Gharaei and S. Mohammadi, Eur. Phys. J. A **55**, 119 (2019).

[25] R. Gharaei, F. K. Najjar, and N. Ghal-Eh, Eur. Phys. J. A **57**, 104 (2021).

[26] I. Dutt and R. Bansal, Chin. Phys. Lett. **27**, 112402 (2010).

[27] I. Dutt and R. K. Puri, Phys. Rev. C **81**, 044615 (2010).

[28] O. N. Ghodsi and A. Daei-Ataollah, Phys. Rev. C **93**, 024612 (2016).

[29] D.-X. Zhu, M. Li, Y.-Y. Xu, X.-J. Wu, B. He, and X.-H. Li, Phys. Scr. **97**, 095304 (2022).

[30] K. P. Santhosha and I. Sukumaran, Eur. Phys. J. A **53**, 136 (2017).

[31] I. Dutt and R. K. Puri, Phys. Rev. C **81**, 047601 (2010).

[32] N. S. Rajeswari and M. Balasubramaniam, J. Phys. G: Nucl. Part. Phys. **40**, 035104 (2013).

[33] N. S. Rajeswari, C. Nivetha, and M. Balasubramaniam, Eur. Phys. J. A **54**, 156 (2018).

[34] D. N. Poenaru, W. Greiner, M. Ivascu, D. Mazilu, and I. H. Plonski, Z. Phys. A **325**, 435 (1986).

[35] G. Audi, F. G. Kondev, M. Wang, W. Huang, and S. Naimi, Chin. Phys. C **41**, 030001 (2017).

[36] W. Huang, G. Audi, M. Wang, F. G. Kondev, S. Naimi, and X. Xu, Chin. Phys. C **41**, 030002 (2017).

[37] M. Wang, G. Audi, F. G. Kondev, W. Huang, S. Naimi, and X. Xu, Chin. Phys. C **41**, 030003 (2017).

[38] V. Y. Denisov and H. Ikezoe, Phys. Rev. C **72**, 064613 (2005).

[39] K. N. Huang, M. Aoyagi, M. H. Chen, B. Crasemann, and H. Mark, At. Data Nucl. Data Tables **18**, 243 (1976).

[40] J. J. Morehead, J. Math. Phys. **36**, 5431 (1995).

[41] I. Dutt, Pramana **76**, 921 (2011).

[42] W. D. Myers and W. J. Swiatecki, Ark. Fys. **36**, 343 (1967).

[43] K. Pomorski and J. Dudek, Phys. Rev. C **67**, 044316 (2003).

[44] G. Royer and B. Remaud, J. Phys. G: Nucl. Phys. **10**, 1057 (1984).

[45] P. Moller and J. R. Nix, Nucl. Phys. A **361**, 117 (1981).

[46] H. J. Krappe, J. R. Nix, and A. J. Sierk, Phys. Rev. C **20**, 992 (1979).

[47] P. Moller, J. R. Nix, W. D. Myers, and W. J. Swiatecki, At. Data Nucl. Data Tables **59**, 185 (1995).

[48] P. Moller and J. R. Nix, Nucl. Phys. A **272**, 502 (1976).

[49] C. Qi, D. S. Delion, R. J. Liotta, and R. Wyss, Phys. Rev. C **85**, 011303(R) (2012).

[50] Z. X. Zhang and J. M. Dong, Chin. Phys. C **42**, 014104 (2018).

[51] I. Sreeja and M. Balasubramaniam, Eur. Phys. J. A **54**, 106 (2018).

[52] J.-L. Chen, J.-Y. Xu, J.-G. Deng, X.-H. Li, B. He, and P.-C. Chu, Eur. Phys. J. A **55**, 214 (2019).

[53] R. Gharaei, M. J. Shakib, and K. P. Santhosh, Nucl. Phys. A **1037**, 122700 (2023).

[54] R. Gharaei, O. N. Ghodsi, and M. H. Kafash, Ann. Phys. (NY) **419**, 168236 (2020).